THE JOURNAL OF BIOLOGICAL CHEMISTRY VOL. 284, NO. 4, pp. 2138–2149, January 23, 2009
Printed in the U.S.A.

# Switch 1 Mutation S217A Converts Myosin V into a Low Duty Ratio Motor*

Received for publication, July 21, 2008, and in revised form, November 5, 2008 Published, JBC Papers in Press, November 12, 2008, DOI 10.1074/jbc.M805530200

**Eva Forgacs[‡1], Takeshi Sakamoto[§2], Suzanne Cartwright[‡], Betty Belknap[‡], Mihály Kovács[§¶], Judit Tóth[§‖], Martin R. Webb[**3], James R. Sellers[§2], and Howard D. White[‡4]**

*From the [‡]Department of Physiological Sciences, Eastern Virginia Medical School, Norfolk, Virginia 23507, the[**]Division of Physical Biochemistry, National Institute of Medical Research, Mill Hill, London NW7 1AA, United Kingdom, the [§]Laboratory of Molecular Physiology, National Institutes of Health, NHLBI, Bethesda, Maryland 20892, the [¶]Department of Biochemistry, Eötvös University, H-1117 Budapest, Hungary, and the [‖]Institute of Enzymology, Biological Research Center, Hungarian Academy of Sciences, H-1113 Budapest, Hungary*

**We have determined the kinetic mechanism and motile properties of the switch 1 mutant S217A of myosin Va. Phosphate dissociation from myosin V-ADP-$P_i$ (inorganic phosphate) and actomyosin V-ADP-$P_i$ and the rate of the hydrolysis step (myosin V-ATP → myosin V-ADP-$P_i$) were all ~10-fold slower in the S217A mutant than in wild type (WT) myosin V, resulting in a slower steady-state rate of basal and filamentous actin (actin)-activated ATP hydrolysis. Substrate binding and ADP dissociation kinetics were all similar to or slightly faster in S217A than in WT myosin V and mechanochemical gating of the rates of dissociation of ADP between trail and lead heads is maintained. The reduction in the rate constants of the hydrolysis and phosphate dissociation steps reduces the duty ratio from ~0.85 in WT myosin V to ~0.25 in S217A and produces a motor in which the average run length on actin at physiological concentrations of ATP is reduced 10-fold. Thus we demonstrate that, by mutational perturbation of the switch 1 structure, myosin V can be converted into a low duty ratio motor that is processive only at low substrate concentrations.**

During the past 2 decades a considerable number of different myosins have been discovered (1). Myosin V is the best characterized among the so-called unconventional myosins (*i.e.* those not belonging to class II), and it serves as an important model molecule for studying actomyosin interactions and single molecule processive motility (2). Myosin V is a highly processive motor whose role is to transport cargo along actin filaments or bundles inside the cell (3–5). The kinetic mechanism of myosin V is significantly different from that of conventional myosins such as muscle myosin II, as it remains bound to actin (filamentous actin) through a number of ATPase cycles (6–8). Myosin V has a high duty ratio: a single-headed myosin V-S1 (myosin V, subfragment 1) is in the strongly bound AM-ADP state 80–90% of the time during ATP hydrolysis. An additional mechanism for promoting highly processive runs is the preferential release of ADP from the trail head because of mechanochemical gating, which causes a drastic reduction of the rate constant of ADP release from the lead head (9–11). Although there are significant differences between the ATPase mechanisms of the different myosins, the structure of the nucleotide binding pocket (composed of the switch 1 and 2 regions and the P-loop) is highly conserved. The position of the $Ser^{217}$ ($Ser^{236}$ in *Dictyostelium* myosin II) residue of the switch 1 loop (the first serine in the NDNSSRFG sequence) is shown in Fig. 1. It had been shown previously by mutagenesis in *Dictyostelium* (12) and in smooth muscle myosin II (13) that the substitution of serine 236 to alanine retains at least partial enzymatic and motile function in these mutant myosins. Therefore, the OH group is not an essential part of the catalytic mechanism, but the rate of steady-state ATP hydrolysis is reduced several fold. However, neither of these studies includes a detailed kinetic analysis to determine which steps of the catalytic mechanism were altered by the mutation. Here we have exploited the higher affinity of myosin V-ADP-$P_i$ for actin to determine the effect of the mutation on the rate constants of the product dissociation steps following the power stroke, which could not be determined using either *Dictyostelium* or smooth muscle myosin. We also conducted single molecule motility studies using total internal reflectance fluorescence (TIRF)[5] microscopy to determine how the changes in the kinetic mechanism affect the motile properties of the molecule.

## EXPERIMENTAL PROCEDURES

*Preparation of WT and S217A Myosin V-S1 and Myosin V-HMM*—Constructs of mouse WT PVL1392 myosin V-S1 (subfragment 1), coding for amino acids 1–907 (6IQ

* This work was supported, in whole or in part, by National Institutes of Health Grant EB00209 (to H. D. W.). The costs of publication of this article were defrayed in part by the payment of page charges. This article must therefore be hereby marked "*advertisement*" in accordance with 18 U.S.C. Section 1734 solely to indicate this fact.
[1] Supported by a postdoctoral fellowship from the American Heart Association.
[2] Supported by a National Institutes of Health grant from the NHLBI Intramural Program.
[3] Supported by the Medical Research Council, UK.
[4] To whom correspondence should be addressed. Tel.: 757-446-5652; Fax: 757-624-2270; E-mail: whitehd@evms.edu.

[5] The abbreviations used are: TIRF, total internal reflectance fluorescence; S1, subfragment 1; HMM, heavy meromyosin; deac-aminoATP, 3′-(7-diethylaminocoumarin-3-carbonylamino)-3′-deoxyadenosine 5′-triphosphate; deac-aminoADP, 3′-(7-diethylaminocoumarin-3-carbonylamino)-3′-deoxyadenosine 5′-diphosphate; mdATP, 3′-*O*-(*N*-methylanthraniloyl)-2′-deoxyadenosine 5′-triphosphate; mdADP, 3′-*O*-(*N*-methylanthraniloyl)-2′-deoxyadenosine 5′-diphosphate; MOPS, 4-morpholinepropanesulfonic acid; PBP, phosphate-binding protein; WT, wild type; MDCC-PBP, *N*-[2-(1-maleimidyl)ethyl]-7-(diethylamino)coumarin-3-carboxamide phosphate binding protein.

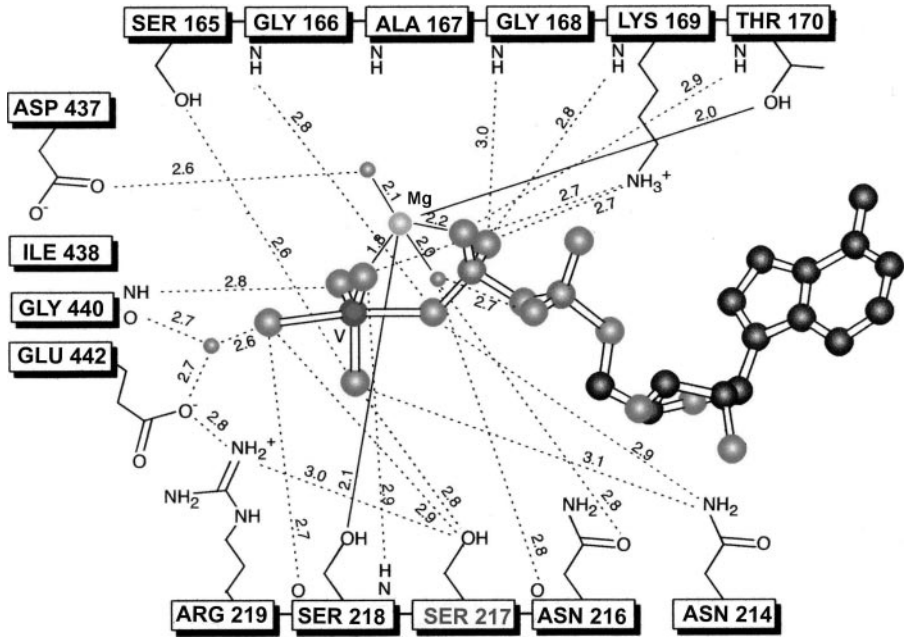


FIGURE 1. **Schematic representation of the critical residues in the ATP binding site of myosin based on the MgADP·$VO_4$ crystal of the *Dictyostelium* motor domain (Smith and *Rayment* (30)).** The serine in position 217 was mutated to alanine for these kinetic studies. The *small spheres* are at the position of the oxygen of the water molecules.

calmodulin binding domains), and heavy meromyosin (HMM), coding for amino acids 1–1090, were used to engineer the mutants. Mutagenesis was performed using the QuikChange site-directed mutagenesis kit (Stratagene). The sequences of the mutant clones were verified by automated fluorescence dye terminator sequencing. The recombinant DNA was transfected into Sf9 insect cells, and the recombinant virus was purified by several rounds of plaque purification. Myosin V-S1 and HMM(S217A) were co-expressed with calmodulin in a baculovirus/Sf9 cell expression system, purified using FLAG affinity chromatography (8), and then concentrated and fractionated on a MonoQ ion exchange column with a linear gradient of 0.1–0.5 M KCl. The protein concentration was determined from $A_{280} - 1.5\ A_{320}$ ($A_{320}$ was subtracted to correct for light scattering) using the extinction coefficients per active site of $\epsilon_{280} = 0.112\ \mu M^{-1}cm^{-1}$ for the S1 and $\epsilon_{280} = 0.120\ \mu M^{-1}\,cm^{-1}$ for the HMM construct calculated from the number of tyrosine and tryptophan residues and their molar extinction coefficients at 280 nm (14). All preparations were analyzed by SDS-protein gel electrophoresis and by active site titration with deac-aminoATP. The protein was stored on ice in buffer containing 10 mM MOPS, 1 mM EGTA, and 400 mM KCl, pH 7.2, and used within 72 h.

*Reagents*—Actin was purified from rabbit skeletal muscle (15). ATP and ADP were purchased from Sigma-Aldrich. *N*-Methylanthraniloyl derivatives of the 2′-deoxynulceotides mdADP and mdATP were synthesized and purified according to the method of Hiratsuka (16). Deac-aminoADP and deac-aminoATP were synthesized by the method of Webb *et al.* (17). Deoxymant nucleotide concentrations were based upon the molar extinction coefficient of $\epsilon_{355} = 5400\ M^{-1}cm^{-1}$ (16), and deac-amino nucleotide concentrations were based upon molar extinction coefficients of $\epsilon_{429} = 46800\ M^{-1}cm^{-1}$ (17).

*Steady-state Basal and Actin-activated ATPase Measurements*—Steady-state ATPase activities were measured by an NADH-coupled assay at 25 °C in buffer containing 10 mM MOPS (pH 7.0), 2 mM $MgCl_2$, 25 mM KCl, 0.15 mM EGTA, 2 mM ATP, 40 units/ml lactate dehydrogenase, 200 units/ml pyruvate kinase, 1 mM phosphoenolpyruvate, and 200 $\mu$M NADH (18). Changes in NADH absorption at 340 nm ($\epsilon_{340} = 6220\ M^{-1}cm^{-1}$) were followed in a Beckman DU640 spectrophotometer. The ATPase activity of blanks containing actin but no myosin was subtracted from the actomyosin data.

*Quench-flow Experiments*—Chemical quench measurements were done using a computer-controlled stepper motor apparatus built in our laboratory (19) to drive syringes in a mixing unit from KinTek Corp. (Austin, TX). Solutions of myosin V (15 $\mu$l) and ATP (10 $\mu$l containing 100,000 dpm of [$\gamma^{32}$P]ATP) were mixed, held in a delay line for the desired time, and then quenched by a second mix with 0.3 M $KH_2PO_4$, 2 N HCl to give a final volume of 1.0 ml. The total radioactivity in each sample was determined by counting 0.3 ml of the sample directly. A 0.6-ml portion of the sample was mixed with an equal volume of a 10% w/v charcoal slurry and spun for 3 min at 10,000 rpm in a tabletop Eppendorf centrifuge to remove unhydrolyzed ATP, and 0.6 ml of the supernatant solution was counted. The percent hydrolysis was obtained from the ratio of the radioactivity in charcoal treated to directly counted samples after subtracting the background from each. The data were then fit to a 2 exponential equation using Simplex fitting routines in Scientist to obtain amplitude and rate information.

*Stopped-flow Experiments*—All stopped-flow measurements were done at 20 °C using an SF-2001 stopped-flow apparatus (KinTek Corp.) fitted with two 2-ml and one 5-ml syringe. The excitation light from a 75-watt xenon lamp was selected by using a 0.2-m monochromator (Photon Technology International, South Brunswick, NJ). deac-aminoATP, deac-aminoADP, and MDCC-PBP were excited at 430 nm, and the emitted light was selected using a 450 nm long-pass filter. In the experiments where deoxymantATP was used, excitation was at 360 nm and emission was selected using a 400 nm long-pass filter. Light scattering was measured by using an excitation wavelength of 450 nm and a 400 nm long-pass filter. Stocks of myosin V(S217A) mutants were diluted from buffer containing 400 mM KCl to obtain the desired protein concentration and a final KCl concentration of 125 mM just prior to use. In double mixing experiments myosin V was mixed with ATP or deac-aminoATP in buffer containing no KCl, incubated for the required time, and then mixed with actin containing the desired nucleotide chase (also in buffer with no KCl). The final concen-

**TABLE 1**

**Summary of kinetic parameters for WT and myosin V (S217A)**

A = Actin, M = myosin V, T = ATP, D = ADP, P = phosphate. Positive (unsigned) lowercase subscripts denote the binding of the last ligand in the subscript to myosin (*e.g.* $k_{AT}$ is the binding of ATP to actomyosin). Negative lowercase subscripts denote dissociation of the last ligand of the substrate from myosin (*e.g.* $k_{-DAP}$ is the dissociation of phosphate from actomyosin V-ADP-$P_i$). Uppercase subscripts denote equilibrium constants (*e.g.* $K_H$ is the equilibrium constant for M-ATP ⇄ M-ADP-$P_i$). Steady-state rates are given per active site. Numbers in parentheses after the rate constants refer to the figures in this manuscript. NS, indicates data reported in the text but not shown in a figure.

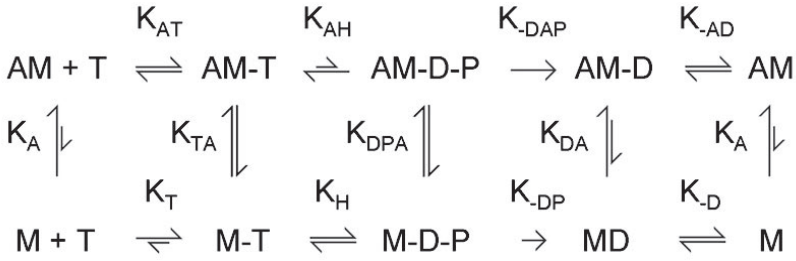


| Kinetic Constant | Method | Nucleotide | S1-WT | S1-S$^{217}$A | HMM-WT | HMM-S$^{217}$A |
|---|---|---|---|---|---|---|
| **Steady-State Kinetics** | | | | | | |
| $k_{-DP}$ ($s^{-1}$) | NADH linked (basal) | ATP | 0.027(NS) | 0.002 (NS) | 0.021 (NS) | 0.0028 (NS) |
| $V_{max}$ ($s^{-1}$) | NADH linked (+actin) | ATP | 12.4 (NS) | 2.7 (NS) | 8.2 (NS) | 1.7 (NS) |
| $K_{ATPase}$ (μM) | NADH linked (+actin) | ATP | 2.6 (NS) | 8.6 (NS) | 0.55 (NS) | 2.5 (NS) |
| **Transient Kinetics** | | | | | | |
| $k_T$ ($\mu M^{-1}s^{-1}$) | SF single turnover | deac-aminoATP | 3.4[a] | 3.2 (2) | 3.5[b] | 3.7 (NS) |
| $k_T$ ($\mu M^{-1}s^{-1}$) | SF tryptophan | ATP | 2.3 (3) | 3.4 (3) | | |
| $k_{AT}$ ($\mu M^{-1}s^{-1}$) | SF light scattering | ATP | - | 0.29 (6) | | |
| $k_H$ ($s^{-1}$) | SF tryptophan | ATP | 84 (3) | 9.9 (3) | | |
| $k_H$ ($s^{-1}$) | QF | ATP | >30 (4) | 8.2 (4) | | |
| $K_H$ | QF | ATP | 4.4 (4) | 4.1 (4) | | |
| $k_{-D}$ ($s^{-1}$) | SF fluorescence | deac-aminoADP | 0.49[a] | 0.86 (7) | | |
| $k_{-AD}$ ($s^{-1}$) | SF fluorescence | deac-aminoATP | 0.52[a] | 1.34 (7) | | |
| $k_{-AD}$ ($s^{-1}$) | SF light scattering | deac-aminoADP | 0.50 (NS) | 0.90 (7) | | |
| $k_{-AD}$ ($s^{-1}$) | SF light scattering | deoxymantATP | 17 (NS) | 20 (7) | | |
| $k_{-AD}$ ($s^{-1}$) | SF light scattering | ADP | 10 (NS) | 17 (7) | | |
| $k_{-AD}$ ($s^{-1}$) | SF double-mixing | deac-aminoATP | 0.48[b] | 0.74 (8) | 0.48[b,d]; 0.015[b,d] | 0.8[d]; 0.01[d] (8) |
| $k_{-DP}$ ($s^{-1}$) | SF single turnover | deac-aminoATP | 0.025[a] | 0.0055 (2) | 0.027 | 0.0053 (NS) |
| $k_{-DAP}$ ($s^{-1}$) | SF MDCC-PBP | ATP | 198[c] | 16 (5) | 228[c] | 21 (7) |

[a] Ref. 22.
[b] Ref. 9.
[c] Ref. 10.
[d] Biphasic kinetics are attributed to strain on the lead head of myosin V-HMM.

tration of buffer in the flow cell was 10 mM MOPS, pH 7.5, 3 mM $MgCl_2$, 25 mM KCl, and 1 mM EGTA. Actin filaments were stabilized with equimolar phalloidin. Stock solutions of actin (80 μM) and ADP (2 mM) were treated for 1 h at 20 °C with 1 mM glucose and 0.01 unit/ml hexokinase to remove traces of ATP in experiments where the actin contained an ADP chase. Phosphate dissociation from the actomyosinADP-$P_i$ complex was measured using MDCC-PBP as described (19). Background $P_i$ was removed by preincubating the stopped-flow apparatus and all working solutions with the phosphate mop consisting of 0.1 mM 7-methylguanosine and 0.01 units/ml purine-nucleoside phosphorylase.

*Single Molecule Motility Assay*—The single molecule motility assay was performed by using TIRF as described previously (20, 21). Calmodulin was labeled with Alexa Fluor 568, exchanged for endogenous calmodulins of WT myosin V-HMM and the S217A mutant, and observed with TIRF using a 532 nm diode laser to excite the Alexa Fluor. Velocity was determined from the time dependence of the movement of the fluorophore using Metamorph software. Average run lengths, $\langle d \rangle$, were determined by fitting the run length data, which had been put in 0.25-μm bins, to single exponential curves (not shown).

*Data Analysis and Kinetic Simulation*—Three to four data traces of 1000 points were averaged, and the observed rate constants were obtained by fitting one or two exponential terms to the data using the software package included with the KinTek stopped-flow instrument. Scientist (Micromath) software was used to replot the data for publication and for kinetic simulations.

## RESULTS

*Steady-state Measurements*—The basal and actin-activated ATPase activities of the myosin V-S1(S217A) and HMM-(S217A) mutants, measured with an NADH-coupled ATP-regenerating system, are summarized in the top two rows of Table 1. WT myosin V-S1 and HMM were used as controls. The hydrolysis rates were determined from the change in absorption at 340 nm, which was linear between 1 and 20 min after initiating the reaction. The basal ATPase activity for both the

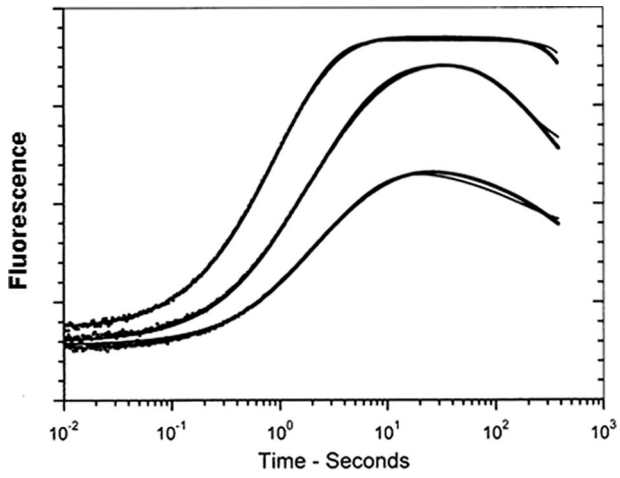


FIGURE 2. **Stopped-flow titration of the Myosin V-S1(S217A) mutant with deac-aminoATP.** Single and multiple turnover stopped-flow measurements were performed by mixing myosin V- S1(S217A) with increasing concentrations of deac-aminoATP. Final concentrations in the cell were 0.12 $\mu$M myosin V-S1(S217A), 0.09, 0.18, and 0.36 $\mu$M deac-aminoATP, 25 mM KCl, 10 mM MOPS, 3 mM $MgCl_2$, 1 mM EGTA, pH 7.5, 20 °C. The *lines* through the data points are global fits to rate constants $k_T = 3.2\ \mu M^{-1}s^{-1}$, $k_{-DAP} = 0.0055\ s^{-1}$.

S1 and HMM mutants was 0.002 and 0.0028 $s^{-1}$ (calculated per active site), which is ~10-fold lower than the values measured for WT myosin V-S1 and HMM. Actin accelerated the ATPase activity of myosin V(S217A) by ~1000-fold, reaching a $V_{max}$ of 2.7 $s^{-1}$ for S1(S217A) and 1.7 $s^{-1}$ for HMM(S217A), which is ~5-fold slower than WT. Half-maximal activation ($K_{ATPase}$) occurred at an actin concentration of 8.6 $\mu$M for the S1 and 2.5 $\mu$M for the HMM mutants. Both were ~3-fold higher than observed for WT (Table 1).

*Single and Multiple Turnover Stopped-flow Measurements of deac-aminoATP Binding to and Hydrolysis by Myosin V-S1(S217A) and HMM(S217A)*—We did single and multiple turnover stopped-flow measurements in which we rapidly mixed myosin V-S1(S217A) and HMM(S217A) (not shown) with different concentrations of deac-aminoATP (Fig. 2). Global fits of the data were used to determine the rate constants of deac-aminoATP binding ($k_T$), the rate-limiting step of steady-state deac-aminoATP hydrolysis ($k_{-DAP}$), and the concentration of active sites. The second order rate constants of deac-aminoATP binding to myosin V(S217A), $k_T$, were 3.2 $\mu M^{-1}s^{-1}$ for S1 and 3.7 $\mu M^{-1}s^{-1}$ for HMM, which are essentially the same as those observed for the WT myosin V-S1 and HMM (9, 22). There is a ~5-fold reduction in the rate of deac-aminoATP hydrolysis to 0.005–0.0055 $s^{-1}$ by myosin V-S1(S217A) and myosin V-HMM(S217A) compared with the rates measured for WT myosin V (9, 22). The concentration of active sites measured by single turnover experiments was 0.9–1.1 times the concentration determined by $A_{280}$, which indicates that the lower rates in the mutants are due to the difference in kinetic properties and not to a reduced fraction of active enzyme molecules.

*ATP Binding and Hydrolysis in the Absence of Actin*—Myosin V and most other myosins have a tryptophan residue ($Trp^{484}$ in myosin V) in the relay loop that is an intrinsic fluorescence sensor of conformational changes occurring in the nucleotide binding pocket resulting from substrate binding and hydrolysis (23–26). We did single mixing stopped-flow experiments in which we mixed apyrase-treated (to ensure that the myosin does not have ADP bound) WT myosin V-S1 or myosin V-S1(S217A) with substoichiometric ATP concentrations (data not shown). The rapid increase in tryptophan fluorescence is the result of ATP binding to myosin V and hydrolysis to myosin V-ADP-Pi, which was followed by a slow decrease produced by the dissociation of phosphate at 0.03 $s^{-1}$ in the WT and 0.002 $s^{-1}$ in the S217A mutant. Data from experiments in which myosin V was mixed with excess ATP were fit by single exponentials (Fig. 3, *A* and *B*). The observed rate constants showed hyperbolic dependence upon ATP concentration (Fig. 3*C*) in which the maximal rate constant was 84 $s^{-1}$ for WT S1 and 9.9 $s^{-1}$ for the S217A mutant. The 8–9-fold decrease suggests that the hydrolysis step ($k_{AH} + k_{-AH}$) is significantly slower in the S217A mutant than in WT myosin V. The initial slope of 2.3 $\mu M^{-1}s^{-1}$ for WT myosin V-S1, which measures the rate constant of ATP binding, is similar to published values (6, 7). A slightly larger rate constant of 3.4 $\mu M^{-1}s^{-1}$ was obtained for the myosin V-S1(S217A) mutant.

*Direct Measurement of ATP Hydrolysis by Quench Flow*—Quench flow is the only method that unambiguously measures the hydrolysis step and does not require any assumptions be made for interpretation of the molecular basis of the signal. Myosin V has been reported previously to have a rapid initial burst corresponding to a rapid (>100 $s^{-1}$) and thermodynamically favorable hydrolysis of ATP in the active site of the enzyme (6). We did single and multiple turnover quenched-flow experiments to determine whether the mutant myosin V-S1 shows a $P_i$ burst and to estimate the $K_H$ in the absence of actin. Under single turnover conditions ([ATP]/[S1] = 0.25) the time course of the hydrolysis can be fit by a double exponential with fast and slow phases having amplitudes of 0.74 and 0.18 for WT myosin V and 0.84 and 0.17 for the S217A mutant, respectively (Fig. 4, *A* and *B*, *solid symbols*). Estimates of ~4 for $K_H$ can be obtained from the ratio of the amplitudes of the rapid and slow phases. Given that the ATP hydrolysis is fast, the rate constants for the fast phase (1.1 $s^{-1}$ for WT myosin V and 0.85 $s^{-1}$ for S217A) are limited by the rate of ATP binding. In experiments in which ATP was in excess ([ATP]/[S1] = 4) the burst phase is smaller for both WT and S217A, and the rate constant of the burst is faster for WT myosin V. The observed rate constants were plotted against the sum of ATP and protein concentrations (Fig. 4*C*). A linear dependence of the hydrolysis rate constant upon ATP concentration to >30 $s^{-1}$ was observed for WT S1, whereas a hyperbolic fit resulted in an extrapolated maximal rate constant of 8.2 $s^{-1}$ for myosin V-S1(S217A). Although the maximum rate of the hydrolytic step was not determined for WT myosin by quench flow, the measured value at the highest applied ATP concentration was more than 5 times higher than for the mutant, and the quench-flow data support the conclusion obtained from Fig. 3 that the ATP hydrolysis step is significantly slower in the S217A mutant. The slow phases are ~10-fold slower for the S217A than the WT, which is consistent with the rates measured by the NADH-coupled steady-state assays, tryptophan fluorescence, and single turnover stopped-flow experiments.

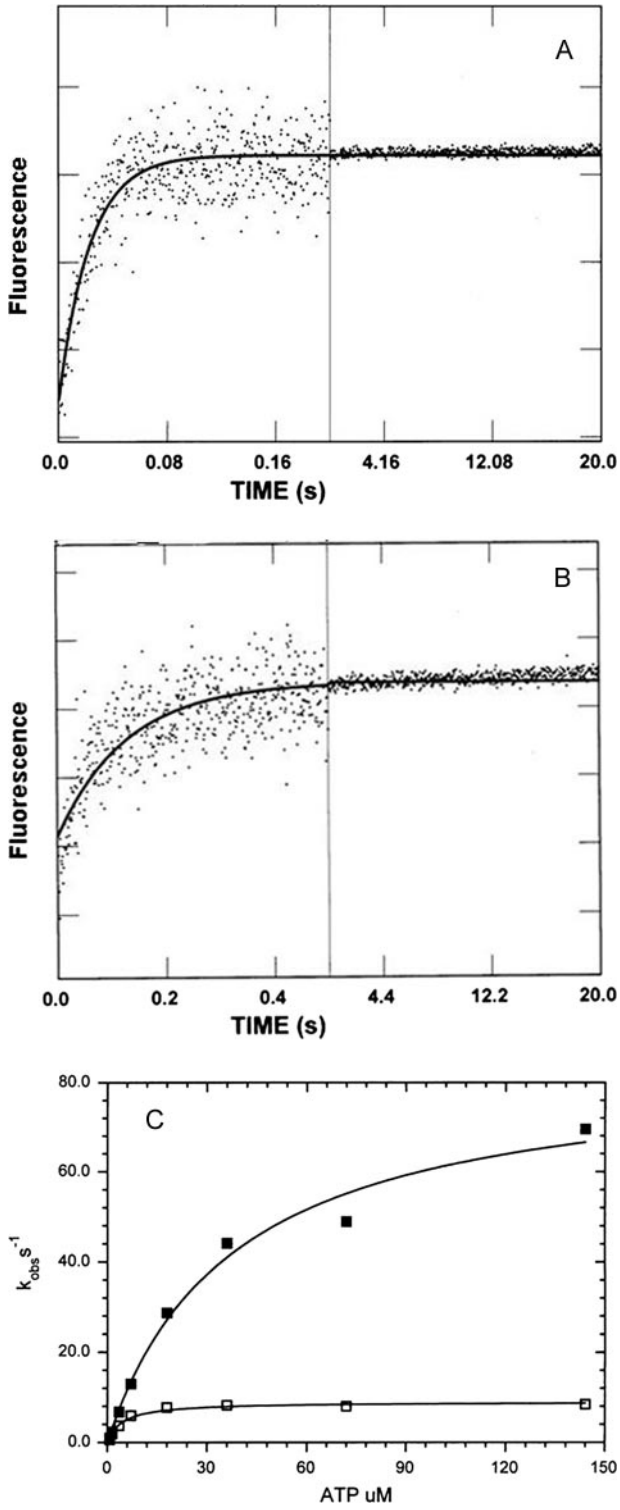


FIGURE 3. **ATP binding and hydrolysis measured by tryptophan fluorescence.** *A*, the increase in tryptophan fluorescence observed upon mixing WT myosin V-S1 with ATP. The *solid line* through the data is the fit to a single exponential equation with a $k_{obs}$ value of 44.1 $s^{-1}$. Experimental conditions were: 0.9 $\mu$M myosin V-S1, 35.8 $\mu$M ATP, 25 mM KCl, 10 mM MOPS, 3 mM $MgCl_2$, 1 mM EGTA, pH 7.5, 20 °C. *B*, conditions were similar to those in *A* except that myosin V-S1(S217A) was used. The data were fit to a single exponential equation with a $k_{obs}$ value of 7.8 $s^{-1}$. *C*, dependence of the observed rate of binding to WT (■) and myosin V-S1(S217A) (□) upon ATP concentration. Experimental conditions were similar to those in *A* and *B* except that the final ATP concentration was varied as indicated. The data are fit to hyperbolas ($k_{obs} = k_{max}/(1 + [ATP]/K_{app})$) with a $k_{max}$ of 84 ± 6 $s^{-1}$ and $K_{app}$ of 37 ± 7 $\mu$M for WT and a $k_{max}$ of 9.9 ± 0.6 $s^{-1}$ and $K_{app}$ of 3.8 ± 0.9 $\mu$M for S217A.

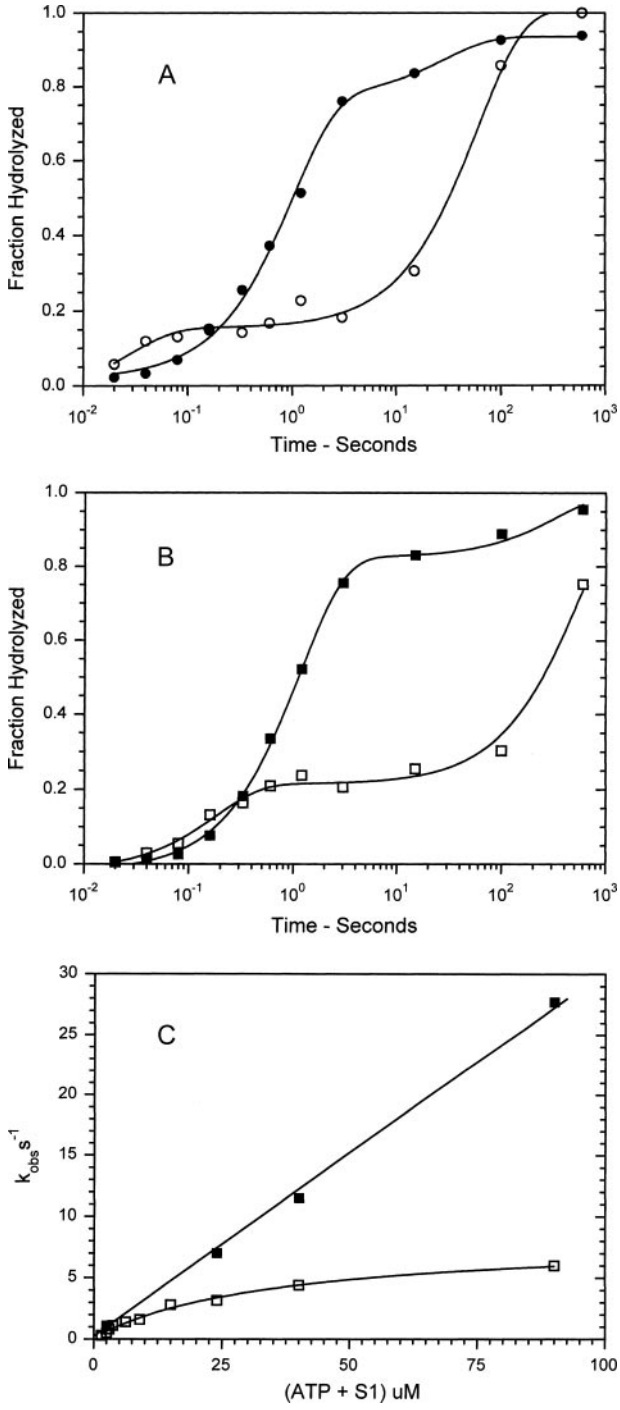


FIGURE 4. **Measurement of ATP hydrolysis by rapid chemical quench.** WT myosin V-S1 (*A*) and myosin V-S1(S217A) (*B*) were mixed with ATP, allowed to react for the indicated amount of time, and then quenched with acid as described under "Experimental Procedures." Final concentrations in the delay line were 4 $\mu$M myosin V-S1 and 1 $\mu$M ATP (●, ■) or 8 $\mu$M S1 and 32 $\mu$M ATP (○, □). The *solid lines* through the data are fits to double exponential equations: *A*, $I(t) = 0.93 - (0.74e^{-1.1\,t} + 0.18e^{-0.03\,t})$ (●) and $I(t) = 1.0 - (0.18e^{-13\,t} + 0.72e^{-0.02\,t})$ (○); *B*, $I(t) = 1.0 - (0.84e^{-0.85\,t} + 0.17e^{-0.003\,t})$ (■) and $I(t) = 0.97 - (0.22e^{6.0+t} + 0.75e^{-0.0023\,t})$ (□). *C*, dependence of the observed rates of hydrolysis upon ATP and S1 concentration. Experiments were similar to those described in *A* and *B* except that the ATP and protein concentrations were varied as indicated. At [S1 + ATP] < 10 $\mu$M, [S1] = 4 × [ATP] and at [S1+ATP] >10 $\mu$M, [ATP] = 4 × [S1]. WT myosin V-S1 (■) are fit by a straight line with a slope of 0.33 ± 0.02 $\mu M^{-1}s^{-1}$. Myosin V(S217A) (□) were fit by a hyperbolic equation in which $k_{max}$ = 8.2 ± 1 $s^{-1}$ and $K_{app}$ = 36 ± 5 $\mu$M.

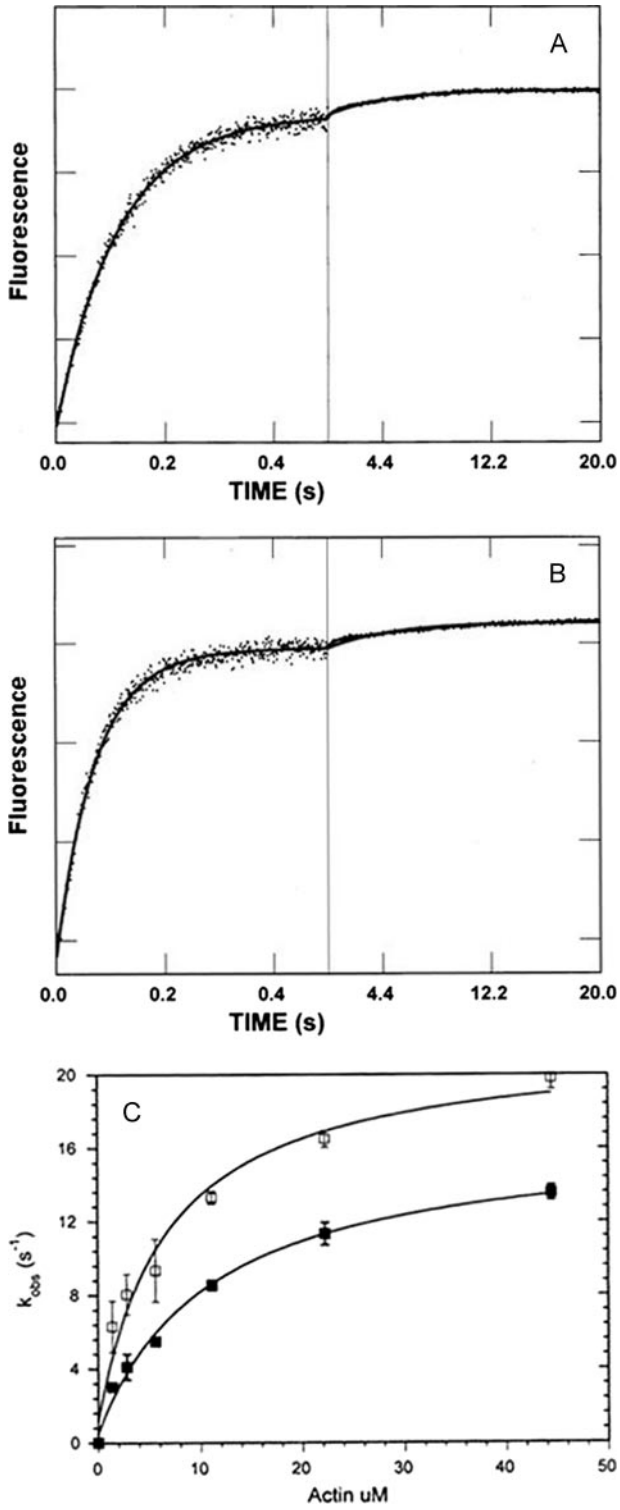


FIGURE 5. **Kinetics of phosphate dissociation from the (acto)myosin V-ADP-$P_i$ complex.** Double mixing stopped-flow experiments using MDCC-PBP were performed as described under "Experimental Procedures." Myosin V-S1(S217A) was first mixed with ATP, held in a delay line for 20 s, and then mixed with actin to accelerate $P_i$ release. Final concentrations in the flow cell were 0.8 $\mu$M myosin V, 0.4 $\mu$M ATP, 0–44 $\mu$M actin, 1 mM EGTA, 3 mM $MgCl_2$, 10 mM MOPS, 25 mM KCl, 10 $\mu$M MDCC-PBP, 0.1 mM 7-methylguanosine, and 0.01 unit/ml purine-nucleoside phosphorylase, pH 7.5, 20 °C. Phosphate dissociation from myosin V-S1(S217A)-ADP-$P_i$ (*A*) and myosin V-HMM(S217A)-ADP-$P_i$ (*B*) complexes in the presence 11.2 $\mu$M actin is shown. The *solid line* through the data is the best fit to a double exponential equation: $I(t) = -(0.19e^{-8.8\,t} + 0.02e^{-0.23\,t}) + C$ for *panel A* and $I(t) = -(0.06e^{-13.9\,t} + 0.006e^{-0.21\,t}) + C$ for *panel B*. *C*, dependence of $k_{obs}$ for phosphate dissociation upon actin concentration were fit by a hyperbolic equation: $k_{obs} = k_{max}/(1 + K_{app}/[actin])$ when $k_{max} = 16 \pm 1.6\ s^{-1}$ and $K_{app} = 9.4 \pm 2.6$ $\mu$M for the myosin V-S1(S217A) (■) and $k_{max} = 20.9 \pm 1.1\ s^{-1}$ and $K_{app} = 5.3 \pm 0.9$ $\mu$M for the myosin V-HMM(S217A) (□).

*Phosphate Dissociation from Actomyosin V-ADP-$P_i$*—The rate constant of phosphate dissociation from the actomyosinADP-$P_i$ complex can be measured by using a fluorescently labeled phosphate-binding protein (MDCC-PBP) (19). In a double mixing stopped-flow experiment, myosin V-S1 or HMM was first mixed with ATP under single turnover conditions and incubated to allow ATP binding and hydrolysis to occur, which was then followed by mixing with actin to measure the kinetics of $P_i$ dissociation. The MDCC-PBP was present at the same concentration in all three syringes, to obtain a large excess over phosphate in the stopped-flow cell. To prevent phosphate contamination, all solutions were preincubated with phosphate mop (for the components and concentrations see "Experimental Procedures"). To obtain the observed rate constants, time courses were fit with double exponential equations. Representative traces are shown in Fig. 5, *A* and *B*. The fast phase had a fractional amplitude of 0.9, which is attributed to the $P_i$ release from the actomyosinADP-$P_i$ complex produced from myosinADP-$P_i$ binding to actin. The slow phase (0.2 $s^{-1}$) had a significantly smaller fractional amplitude (0.09), and based on our previous work with skeletal myosin (10, 19), it measures the rate constant of ATP hydrolysis by myosin V-ATP bound to actin. A hyperbolic fit of the dependence of $k_{obs}$ for the faster phase of $P_i$ dissociation upon actin concentration has a maximal rate of 16.2 ± 1.6 $s^{-1}$ and an apparent actin dissociation constant of 9.4 ± 2.6 $\mu$M for the actomyosin V-S1(S217A)ADP-$P_i$ products (Fig. 5*C*). A similar maximum phosphate dissociation rate of 21 ± 1 $s^{-1}$ and a $K_{app}$ of 5.3 ± 0.9 $\mu$M were obtained for the myosin V-HMM(S217A) (Fig. 5*C*). The rate constants of $P_i$ dissociation measured here for myosin V(S217A) are ~10 times less than the rate constants measured for WT myosin V-S1 and HMM as reported previously (4, 10, 22).

*ATP Induced Dissociation of Actomyosin V-S1(S217A)*—ATP binding to the actomyosin complex induces a conformational change that results in weaker binding and subsequent dissociation of most types of myosin from actin. We measured the decrease in light scattering following mixing actomyosin V-S1(S217A) with ATP, which was fit by two exponential terms (Fig. 6*A*). A linear fit of the dependence of the faster rate upon ATP concentration gives a second order rate constant of 0.29 $\mu M^{-1}s^{-1}$ (Fig. 6*B*). The end point of the light-scattering signal observed upon mixing actomyosin V-S1(S217A) with ATP is approximately half-way between light scattering of the actomyosin V-S1(S217A) and the light-scattering signal from actin in the absence of myosin V-S1. These experiments indicate that at the end of the rapid phase myosin V-S1(S217A) is only ~50% dissociated from 5 $\mu$M actin. The $K_{app}$ is, therefore, ~5 $\mu$M for myosin V-S1(S217A)-ATP binding to actin. The relatively small amplitude of the slow phase indicates that there is not a significant change in the affinity of the myosin for actin associated with the hydrolysis step. Because the rates of hydrolysis, phosphate dissociation, and ADP dissociation are similar, it

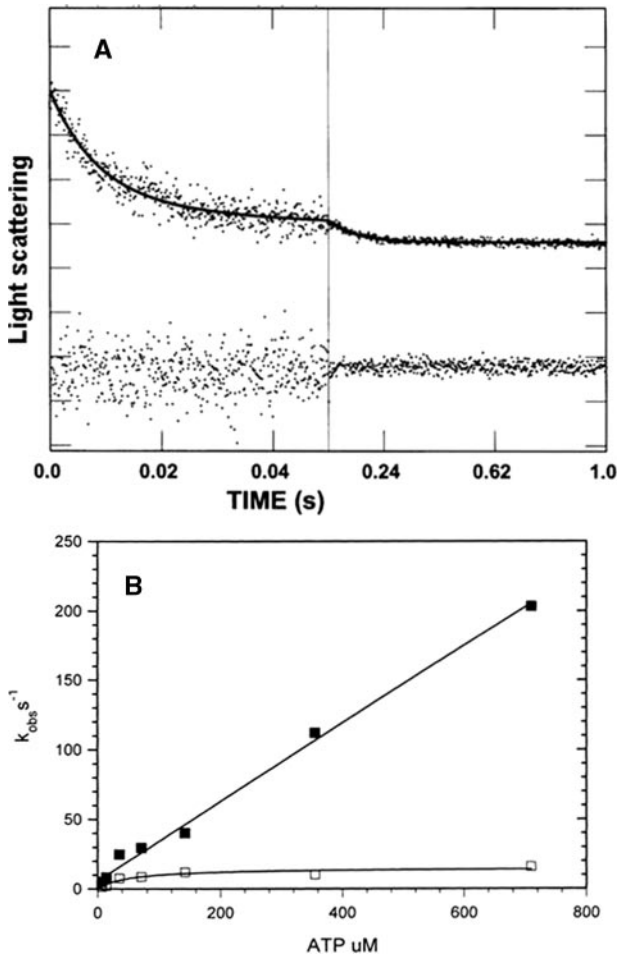


FIGURE 6. **ATP induced dissociation of myosin V-S1(S217A) from actin.** *A*, the *upper curve* shows the decrease in light scattering observed upon mixing actomyosin V-S1(S217A) with ATP. The *solid line* through the data is a fit to $I(t) = 0.05e^{-112+t} + 0.01e^{-10.2\,t} + C$. The *lower curve* was obtained by mixing actin alone with ATP. Experimental conditions in the flow cell were: 0.5 $\mu$M myosin V-S1(S217A), 5.0 $\mu$M actin, and 358 $\mu$M ATP (final concentrations in the cell), 25 mM KCl, 10 mM MOPS, 3 mM $MgCl_2$, 1 mM EGTA, pH 7.5, 20 °C. *B*, experimental conditions were the same as in *A* except that the ATP concentrations were varied from 7 to 714 $\mu$M. The fast rates (■) were fit by a linear equation with a slope of 0.29 $\mu M^{-1}s^{-1}$, and the slow rates (□) were fit by a hyperbolic equation in which $k_{max} = 18 \pm 7\ s^{-1}$, $K_{app} = 71 \pm 93\ \mu$M.

would be expected that actomyosin V-S1(S217A) intermediates with bound ATP, ADP-$P_i$, and ADP would all be present during the steady state. The maximum rate constant of the fast phase is attributed to the dissociation of myosin V-S1(S217A)-ATP from the actin. The maximum rate constant of the slow phase, 18 $s^{-1}$, is in reasonably good agreement with the modeled rate of 24 $s^{-1}$ at which a reaction with a hydrolysis rate constant of 8 $s^{-1}$ and a phosphate dissociation rate constant of 16 $s^{-1}$ approaches the steady-state binding of myosin V-S1(S217A) to actin after mixing actomyosin with ATP. We could not observe a change in light scattering for WT actomyosin V-S1 because of the tight binding of myosin V to actin in the presence of ATP (data not shown).

*ADP Dissociation from Myosin V-S1(S217A) in the Absence and Presence of Actin*—The dissociation of deac-aminoADP from the S1(S217A) was measured by mixing the myosin V-S1(S217A)-deac-aminoADP complex with excess ATP. A rate constant of 0.86 $s^{-1}$ was obtained by fitting a single exponential to the fluorescence decrease (Fig. 7*A*). The rate constant of deac-aminoADP dissociation from actomyosin V-S1(S217A)-deac-aminoADP was determined to be 1.34 $s^{-1}$ in an experiment in which the initial mixture of actin, myosin V-S1(S217A), and deac-aminoADP were mixed with ATP (Fig. 7*B*). The dissociation of ADP, deoxymantADP, and deac-aminoADP from actomyosin V-S1(S217A) was also measured by light scattering. Actomyosin V-S1(S217A)-ADP complexes were mixed with ATP, and the rate constant of ADP dissociation was determined using light scattering to measure the rate at which excess ATP dissociated the myosin V from actin. Dissociation rate constants of 17 $s^{-1}$ (ADP), 20 $s^{-1}$ (mdADP), and 0.9 $s^{-1}$ (deac-aminoADP) were measured for dissociation of nucleoside diphosphates from actomyosin V-S1(S217A) (Fig. 7, *C–E*). Rate constants of 10, 17, and 0.5 $s^{-1}$ were measured for the dissociation of the same series of nucleotide diphosphates from WT actomyosin V-S1 (data not shown). These experiments show that ADP, deoxymantADP, and deac-aminoADP dissociation occurs at a slightly higher rate from the actomyosin V-S1(S217A) than from WT actomyosin V-S1 complexes (22).

*Measurement of deac-aminoADP Dissociation from Actomyosin V-deac-aminoADP-$P_i$ Complexes*—We used double mixing stopped-flow experiments to measure the rate constants of the deac-aminoADP dissociation from the actomyosin V-HMM(S217A)-deac-aminoADP-$P_i$ complex and to determine whether the dissociation rate from the lead head is reduced in S217A as was observed previously in the WT. Equimolar concentrations of mutant myosin V-S1 or HMM and deac-aminoATP were mixed, and the reaction was aged for 20 s to allow deac-aminoATP to bind and be hydrolyzed by myosin V. The kinetics of product dissociation were measured after a second mix with phalloidin-actin and either a 2 mM ATP chase or a 2 mM hexokinase-treated ADP chase to prevent deac-aminoADP rebinding. When myosin V-HMM(S217A) and an ATP chase were used, we observed a single phase with a rate constant of 0.64 $s^{-1}$ (Fig. 8*A*). The ATP chase rapidly dissociates the empty trail head after product dissociation, thereby abolishing the strain-induced inhibition of ADP dissociation from the lead head (9). When ADP was used as a chase the reaction was biphasic with a faster rate constant of 0.8 $s^{-1}$ (fractional amplitude, 0.7) and a slower rate constant of 0.01 $s^{-1}$ (fractional amplitude, 0.3) (Fig. 8*B*). With the ADP chase the faster component can be attributed to deac-aminoADP dissociation from the trail head and the slower rate constant to the deac-aminoADP dissociation from the lead head, similar to what was observed for the WT myosin V-HMM (9). As expected, the reaction was also monophasic when myosin V-S1(S217A) was used with an ADP chase and gave a $k_{obs}$ of 0.74 $s^{-1}$ (Fig. 8*C*).

*Single Molecule Motility Assay*—TIRF assays were conducted using WT and mutant myosin V-HMM in which the endogenous calmodulin was exchanged for Alexa Fluor 568-calmodulin, and the labeled molecules were observed by exciting the fluorophore with a 532 nm laser. The myosinV-HMM(S217A) mutant showed a slightly reduced maximum velocity of 485 nm/s compared with the WT, which had a maximum velocity of 695 nm/s (Fig. 9*A*). At saturating ATP (>250 $\mu$M) the run

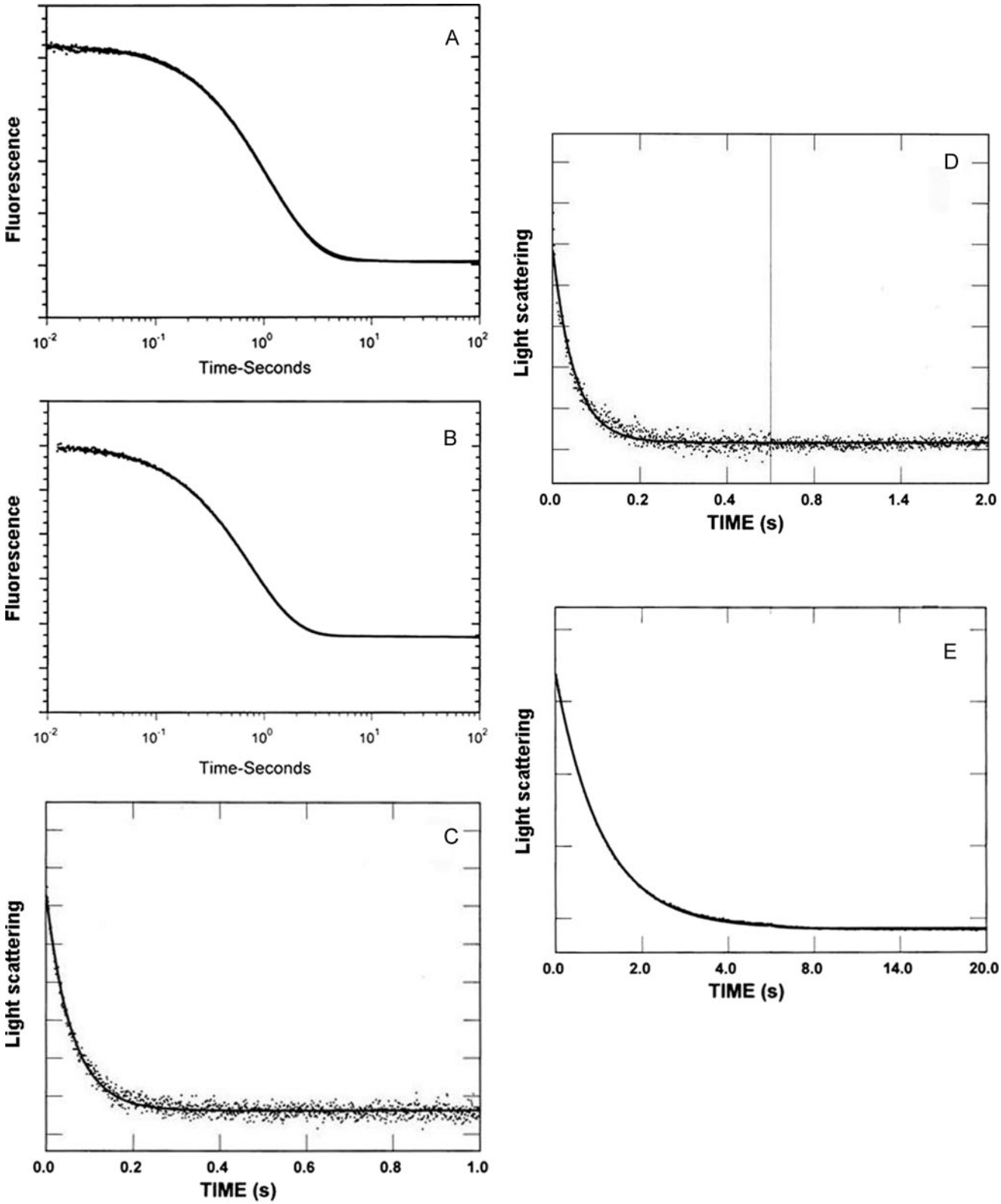


FIGURE 7. **Kinetics of nucleoside diphosphate dissociation from the myosin V-S1(S217A) and actomyosin V-S1(S217A)-ADP complexes.** *A*, a solution containing myosin V-S1(S217A) and deac-aminoADP was mixed with ATP in the stopped-flow apparatus. Final concentrations in the flow cell were: 0.3 $\mu$M myosin V-S1(S217A), 1.4 $\mu$M deac-aminoADP, 1.42 mM ATP, 25 mM KCl, 10 mM MOPS, 3 mM $MgCl_2$, 1 mM EGTA, pH 7.5, 20 °C. The decrease in fluorescence was fit by a single exponential with a $k_{obs} = 0.86\ s^{-1}$. *B*, conditions were similar to those in *A* except that the initial actomyosin V-S1(S217A)-deacaminoADP was formed by the addition of 14.2 $\mu$M phalloidin-actin. The data were fit by a single exponential equation in which $k_{obs} = 1.34\ s^{-1}$, *C–E*, the dissociation of ADP, deoxymantADP, and deac-aminoADP from actomyosin V-S1(S217A) was measured from the decrease in light scattering observed upon mixing the actomyosin V-S1(S217A) nucleotide diphosphate complexes with ATP. The *solid lines* through the data correspond to a $k_{obs}$ of 17, 20, and 0.93 $s^{-1}$ for the dissociation of ADP, deoxymantADP, and deac-aminoADP, respectively. Final concentrations in the flow cell were 0.3 $\mu$M myosin V-S1(S217A), 1.42 $\mu$M nucleoside diphosphate, 0.7 $\mu$M phalloidin-actin, 0.7 mM ATP, 25 mM KCl, 10 mM MOPS, 3 mM $MgCl_2$, 1 mM EGTA, pH 7.5, 20 °C.

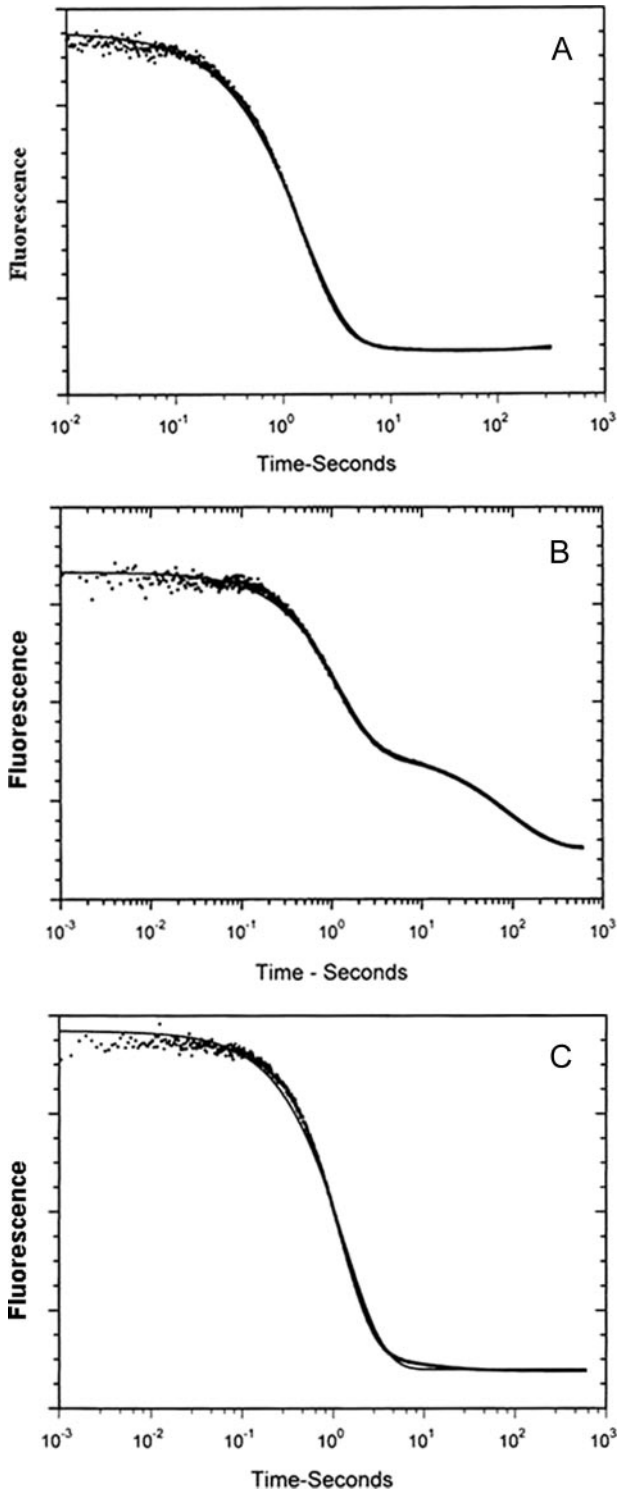


FIGURE 8. **Product dissociation from the actomyosin V-S1(S217A) and actomyosin V-HMM(S217A)-deac-aminoADP-$P_i$ complexes.** *A*, myosin V-HMM(S217A) was mixed with 1 $\mu$M deac-aminoATP, held for 20 s in a delay line, and then mixed with phalloidin-actin and ATP. Experimental conditions: 25 mM KCl, 10 mM MOPS, 3 mM $MgCl_2$, 1 mM EGTA, pH 7.5, 20 °C. Final concentrations in the cell: 0.3 $\mu$M myosin V-HMM(S217A) active sites, 0.3 $\mu$M deac-aminoATP, 11.1 $\mu$M actin, and 1.1 mM ATP. The *solid line* through the data is the best fit to a single exponential equation: $I(t) = 0.65e^{-0.64\,t} + C$. *B*, experimental conditions were similar to those in *A* except that a hexokinase-treated ADP chase replaced ATP: $I(t) = 0.38e^{-0.80\,t} + 0.18e^{-0.010t} + C$. *C*, experimental conditions were similar to those in *B* except that myosin V-S1(S217A) replaced myosin V-HMM(S217A): $I(t) = 0.647e^{-0.74\,t} + C$.

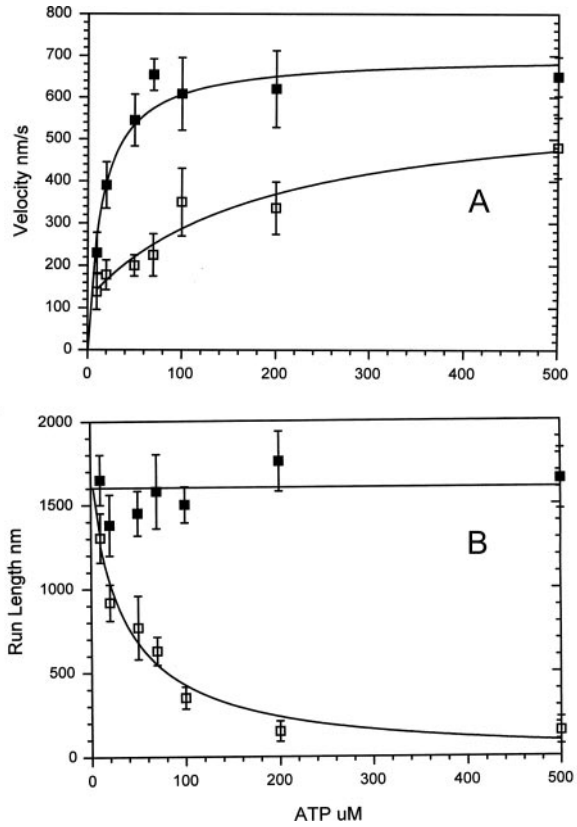


FIGURE 9. **Single molecule motility assay with WT myosin V-HMM and myosin V-HMM(S217A).** Calmodulin was labeled with Alexa Fluor 568 and exchanged for endogenous calmodulins into myosin V-HMM, and the molecule was observed using a 532 nm diode laser. Experimental conditions: 40 mM KCl, 20 mM MOPS, 4 mM $MgCl_2$, 0.1 mM EGTA, 1 $\mu$M calmodulin, 50 mM dithiothreitol, and various concentrations of ATP as indicated at pH 7.5, 25 °C. The reactions also included an oxygen scavenging system composed of 25 $\mu$g/ml glucose oxidase, 45 $\mu$g/ml catalase, and 2.5 mg/ml glucose. *A*, velocity was measured for the movement of WT myosin V-HMM (■) and myosin V-HMM(S217A) (□) on actin at various ATP concentrations. The maximum velocity was 695 nm/s for WT and 485 nm/s for S217A. *B*, run length of WT myosin V-HMM (■) and myosin V-HMM(S217A) (□) at various ATP concentrations. Each data point was obtained by fitting a histogram of the run lengths with a single exponential.

length was reduced by ~10-fold (Fig. 9*B*). However, at low ATP concentrations, the run length measured for myosin V(S217A)-HMM approached that of the WT myosin V.

## DISCUSSION

The active site is highly conserved within the different classes of myosins. It is, therefore, not surprising that site-directed mutagenesis of the active site often produces mutant molecules that are either catalytically inactive or do not function as motor proteins. However, small changes to the active site produce molecules that have altered kinetic properties and provide a useful approach to understanding myosin motor function. Studies in which the first serine in the switch 1 sequence of smooth muscle myosin (13) and in *Dictyostelium* (12) were mutated to alanine suggest that the rate of the product dissociation steps were reduced, but it could not be determined which step(s) of the mechanism had been altered. Myosin V provides an ideal system for kinetic, structural, and motility studies of myosin motor function. The crystal structure of myosin V has been solved in the apoform and several nucleotide-bound

forms (27, 28), and the kinetic mechanism of both the single- and double-headed myosin V has been determined in considerable detail (6, 9, 10, 22). In addition, a number of studies have revealed that myosin Va walks along actin filaments in a hand-over-hand manner with 36-nm processive steps (4, 5, 29).

The OH group of serine 217 in the active site of myosin forms hydrogen bonds with the γ-phosphate of ATP and the $NH_2$ group of $Arg^{219}$ (Fig. 1) (28, 30, 31). Therefore, it was plausible that the removal of the OH group by mutating the serine to alanine would perturb these interactions and would have a detrimental, possibly even lethal, effect on the ATPase mechanism. We carried out a detailed kinetic study to determine the effect of the serine to alanine mutation on the ATPase mechanism and motility. Both the basal and actin-activated steady-state rates were reduced by 5–10-fold. The rate of phosphate dissociation from myosin V(S217A)-ADP-$P_i$ and actomyosin-(S217A)-ADP-$P_i$ were reduced 10-fold as compared with WT, but actin activated the rate of $P_i$ dissociation from both myosin V(S217A) and WT myosin V by ~$10^4$-fold. These data suggest that the mutation either decreases the rate of dissociation by directly changing the interaction between the active site and the phosphate by a local environmental or steric effect or by shifting the equilibrium between conformers of myosin with different affinities for phosphate. Although we do not know why the rate constants of the hydrolysis and phosphate dissociation steps of the reaction were reduced 10-fold or why they still occurred at a reduced rate, a possible explanation is that a water molecule fills the pocket vacated by the serine oxygen and the slightly altered position reduces the rates of both processes.

A second major change in the hydrolysis mechanism is a ~10-fold decrease in the rate of the hydrolysis step measured directly by chemical quench and indirectly by the change in the rate of tryptophan fluorescence. However, the equilibrium constant of the hydrolysis step was unchanged (see Fig. 4), indicating that the rates were changed by equal amounts in both the forward and reverse directions. We were initially surprised by the similar decreases in both the rates of phosphate dissociation and the hydrolysis step. However, the conformational events that must occur in myosin for the power stroke are essentially the same as those that must occur during the reverse of the hydrolysis step, except that one (the power stroke) occurs while bound to actin and the other occurs in the absence of actin (32). It is, therefore, perhaps not surprising that a mutation that affects phosphate dissociation might also affect the observed rate of the hydrolysis step.

The changes in the rate of ATP binding to and the dissociation of ADP and ADP analogues from myosin V and actomyosin V were very small, increasing by less than a factor of 2. Moreover, the strain- induced gating mechanism, which reduces the rate of dissociation of ADP from the lead head of actomyosin V following a power stroke (9, 10), was essentially unchanged by the S217A mutation.

Calculation of the duty ratio has been used to compare the fraction of time that different myosins are in strongly bound actomyosin intermediates (AM and AM-ADP) relative to the weakly bound intermediates (AM-ATP and AM-ADP-$P_i$) (37). The duty ratio, determined by the flux into and out of the strongly bound actomyosin intermediates ($k_{in}/(k_{out}+k_{in})\,k_{in}$, is limited by the rates of hydrolysis ($k_{+H}$) and phosphate dissociation ($k_{-DAP}$), which is equal to $k_{+H}k_{-DAP}/(k_{+H}+k_{-DAP})$. At saturating concentrations of ATP, $k_{out}$ is limited by the rate of ADP dissociation ($k_{-AD}$) from AM-ADP and the rate of M-ATP dissociation from actin ($k_{-TA}$), but the latter is much more rapid for most myosins including myosin V and does not significantly affect the duty ratio. Equation 1 shows the dependence of the duty ratio upon the rate constants of the kinetic mechanism as defined in Table 1.

$$d_{ratio} = \left(\frac{k_{+H}k_{-DAP}}{k_{+H}+k_{-DAP}}\right) \Big/ \left(\left(\frac{k_{+H}k_{-DAP}}{k_{+H}+k_{-DAP}}\right) + k_{-AD}\right) \quad \text{(Eq. 1)}$$

The duty ratio calculated for myosin V decreases from ~0.85 for WT to ~0.25 in myosin V(S217A). It would be expected that the S217A mutation would reduce the processivity of myosin V in the presence of saturating concentrations of ATP by increasing the amount of the hydrolysis cycle spent in weakly bound actomyosin intermediates that could terminate a processive run. The effect of decreasing the rate constants of hydrolysis and phosphate dissociation upon processive movement is visualized in a schematic representation of the myosin V ATP hydrolysis mechanism in Fig. 10, which is based on previous presteady state and single molecule kinetic measurements (9, 10, 33–36). In WT myosin V-HMM, all of the kinetic steps are rapid except for dissociation of ADP from the trail head (Fig. 10, **1** → **2**), which is rate-limiting. At physiological concentrations of ATP this is followed by three rapid steps, ATP binding to the trail head, dissociation of the trail head from actin, and movement of the trail head to become the new lead head (**2** → **3** → **4** → **5**) (11). Hydrolysis of ATP on the lead head occurs prior to binding of the lead head to actin. Intermediate **6**, which has ADP bound to the active site of the head bound to actin and ADP and $P_i$ bound to the dissociated head, is partitioned between intermediates **1** and **7** by the ratio of the rate constants for phosphate dissociation from the lead head (M-ADP-$P_i$) and ADP dissociation from the trail head. For WT myosin V, the rate of phosphate dissociation from the lead head (**6** → **1**) is ~20 times faster than the rate of ADP dissociation from the trail head (**6** → **7**). Intermediate **1**, in which both heads contain bound ADP, is on a path for continued processive motion, whereas intermediate **7** is potentially dissociated by ATP binding to the trail head via intermediates **7** → **8** → **9**. It would therefore be expected that WT myosin V would be partitioned via intermediate **1** more than 95% of the time and produce average processive run lengths of greater than 20 steps, as observed. On the other hand, ADP dissociation from the trail head and phosphate dissociation from the lead head (**6** → **7** and **6** → **1**) have similar rates for the S217A mutant, and the flux of the reaction would be split equally between intermediates **7** and **1**. At high ATP concentrations, ATP binding to the trail head of intermediate **7** produces intermediate **8**, which would have a high probability of dissociating from actin. However, at low concentrations of ATP, intermediate **7** is partitioned primarily to **2**, and processive movement

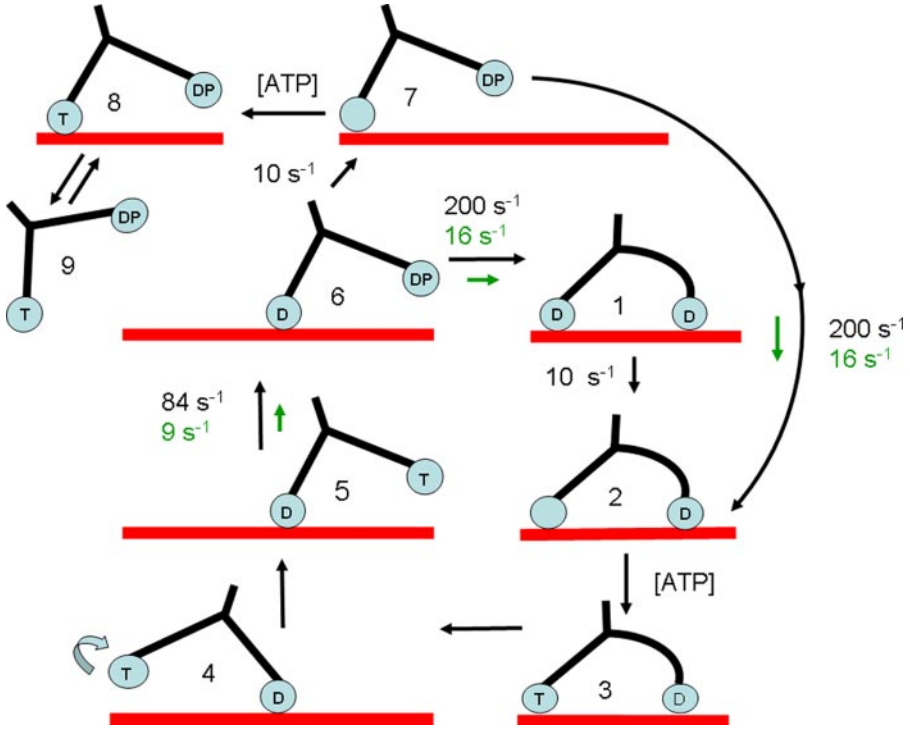


FIGURE 10. **Comparison of the mechanisms of processive movement by WT myosin V and myosin V(S217A) on actin.** Actin is depicted by a *red bar*. Myosin V is moving from *left* to *right*. *T* = ATP, *P* = phosphate, and *D* = ADP. Rate constants measured in this work for myosin V(S217A), which have been observed to be significantly different than WT, are shown in *green* and can be compared with rate constants for WT myosin V, shown in *black*. Second order binding of ATP to myosin is indicated by [ATP]. Rate constants, shown by *single arrows*, are either rapid (>1000 $s^{-1}$) or differ by less than a factor of 2 for WT and S217A.

would continue. This was indeed the case, as very few myosin V-HMM(S217A) were seen bound to actin in a TIRF microscope under high substrate conditions (>250 $\mu$M MgATP). However, WT myosin V moved with an average run length of 1.6 $\mu$m corresponding to forty-four 36-nm steps. Myosin V(S217A) has a run length similar to WT at low substrate concentrations, which increases the amount of time that the trail head remains attached to actin in the rigor form. At MgATP > 250 $\mu$M, the run length of myosin V(S217A) decreases 10-fold to 0.15 $\mu$m, corresponding to an average of four 36-nm steps. These results demonstrate the critical importance of forming a strongly bound lead head at a rate that is substantially faster than the rate at which the trail head is dissociated from actin to maintain processive movement and avoid dissociation of the myosin from actin. We have recently shown the importance of such a mechanism by direct measurements of substrate binding and product dissociation from WT myosin V while it is moving on actin (11). In myosin(S217A) 10-fold reductions in the rate constants of hydrolysis and phosphate dissociation result in a 10-fold reduction of the number of processive steps and the distance that myosin travels on actin before dissociating from it. At low concentrations of ATP, processive motility is restored by reducing the rate at which the trail head is dissociated from actin and allows more time for the lead head to become strongly bound to actin. The reduction in the rate of ADP dissociation from the lead head relative to the trail head, shown in Fig. 8, which has also been proposed to have a major role in processive movement, is essentially unchanged in myosin V(S217A). We have shown that shortening the lever arm by reducing the number of IQ domains to four increased the rate of ADP dissociation from the lead head by 10-fold but had very little affect on processivity (20).[6] Thus, the partitioning of intermediate **6** (Fig. 10) is the predominant factor determining processive movement, and the gating of ADP dissociation may only have a minor role.

In summary, we have shown that the removal of the OH group of the first serine of switch 1 in myosin V markedly decreases the rate constants of ATP hydrolysis and phosphate release, whereas the mutant myosin retains the gated ADP dissociation kinetics of the WT molecule. These kinetic alterations lead to greatly reduced processivity in the mutant enzyme. Our results demonstrate that small structural perturbations can be applied to selectively reduce motor processivity without drastically changing the force-generating and translocating capabilities. Engineered mutations of this sort may become highly useful tools for the selective investigation of the role of processive motility in cellular processes.

*Acknowledgments—We thank Barbara Conyers and Marissa Tribby for excellent technical assistance.*

## REFERENCES

1. Odronitz, F., and Kollmar, M. (2007) *Genome Biol.* **8,** R196
2. Sellers, J. R., and Veigel, C. (2006) *Curr. Opin. Cell Biol.* **18,** 68–73
3. Wu, X., Bowers, B., Wei, Q., Kocher, B., and Hammer, J. A., III (1997) *J. Cell Sci.* **110,** 847–859
4. Mehta, A. D., Rock, R. S., Rief, M., Spudich, J. A., Mooseker, M. S., and Cheney, R. E. (1999) *Nature* **400,** 590–593
5. Yildiz, A., Forkey, J. N., McKinney, S. A., Ha, T., Goldman, Y. E., and Selvin, P. R. (2003) *Science* **300,** 2061–2065
6. De La Cruz, E. M., Wells, A. L., Rosenfeld, S. S., Ostap, E. M., and Sweeney, H. L. (1999) *Proc. Natl. Acad. Sci. U. S. A.* **96,** 13726–13731
7. Trybus, K. M., Krementsova, E., and Freyzon, Y. (1999) *J. Biol. Chem.* **274,** 27448–27456
8. Wang, F., Chen, L., Arcucci, O., Harvey, E. V., Bowers, B., Xu, Y., Hammer, J. A., III, and Sellers, J. R. (2000) *J. Biol. Chem.* **275,** 4329–4335
9. Forgacs, E., Cartwright, S., Sakamoto, T., Sellers, J. R., Corrie, J. E., Webb, M. R., and White, H. D. (2008) *J. Biol. Chem.* **283,** 766–773
10. Rosenfeld, S. S., and Sweeney, H. L. (2004) *J. Biol. Chem.* **279,** 40100–40111
11. Sakamato, T., Webb, M. R., Forgacs, E., White, H. D., and Sellers, J. R. (2008) *Nature* **455,** 128–132

[6] O. Oke, E. Forgacs, T. Sakamoto, M. R. Webb, J. R. Sellers, S. Burgess, P. Knight, H. D. White, and J. Trinick, manuscript in preparation.

12. Shimada, T., Sasaki, N., Ohkura, R., and Sutoh, K. (1997) *Biochemistry* **36,** 14037–14043
13. Li, X. D., Rhodes, T. E., Ikebe, R., Kambara, T., White, H. D., and Ikebe, M. (1998) *J. Biol. Chem.* **273,** 27404–27411
14. Gill, S. C., and von Hippel, P. (1989) *Anal. Biochem.* **182,** 319–326
15. Spudich, J. A., and Watt, S. (1971) *J. Biol. Chem.* **246,** 4866–4871
16. Hiratsuka, T. (1983) *Biochim. Biophys. Acta* **742,** 496–508
17. Webb, M. R., Reid, G. P., Munasinghe, V. R., and Corrie, J. E. (2004) *Biochemistry* **43,** 14463–14471
18. Trentham, D. R., Bardsley, R. G., Eccleston, J. F., and Weeds, A. G. (1972) *Biochem. J.* **126,** 635–644
19. White, H. D., Belknap, B., and Webb, M. R. (1997) *Biochemistry* **36,** 11828–11836
20. Sakamoto, T., Wang, F., Schmitz, S., Xu, Y., Xu, Q., Molloy, J. E., Veigel, C., and Sellers, J. R. (2003) *J. Biol. Chem.* **278,** 29201–29207
21. Sakamoto, T., Yildez, A., Selvin, P. R., and Sellers, J. R. (2005) *Biochemistry* **44,** 16203–16210
22. Forgacs, E., Cartwright, S., Kovacs, M., Sakamoto, T., Sellers, J. R., Corrie, J. E., Webb, M. R., and White, H. D. (2006) *Biochemistry* **45,** 13035–13045
23. Batra, R., and Manstein, D. J. (1999) *Biol. Chem.* **380,** 1017–1023
24. Yengo, C. M., Chrin, L. R., Rovner, A. S., and Berger, C. L. (2000) *J. Biol. Chem.* **275,** 25481–25487
25. Park, S., and Burghardt, T. P. (2000) *Biochemistry* **39,** 11732–11741
26. Malnasi-Csizmadia, A., Woolley, R. J., and Bagshaw, C. R. (2000) *Biochemistry* **39,** 16135–16146
27. Coureux, P. D., Wells, A. L., Menetrey, J., Yengo, C. M., Morris, C. A., Sweeney, H. L., and Houdusse, A. (2003) *Nature* **425,** 419–423
28. Coureux, P. D., Sweeney, H. L., and Houdusse, A. (2004) *EMBO J.* **23,** 4527–4537
29. Walker, M. L., Burgess, S. A., Sellers, J. R., Wang, F., Hammer, J. A., III, Trinick, J., and Knight, P. J. (2000) *Nature* **405,** 804–807
30. Smith, C. A., and Rayment, I. (1996) *Biochemistry* **35,** 5404–5417
31. Fisher, A. J., Smith, C. A., Thoden, J. B., Smith, R., Sutoh, K., Holden, H. M., and Rayment, I. (1995) *Biochemistry* **34,** 8960–8972
32. Lymn, R. W., and Taylor, E. W. (1971) *Biochemistry* **10,** 4617–4624
33. Vale, R. D. (2003) *J. Cell Biol.* **163,** 445–450
34. Purcell, T. J., Morris, C., Spudich, J. A., and Sweeney, H. L. (2002) *Proc. Natl. Acad. Sci. U. S. A.* **99,** 14159–14164
35. Veigel, C., Wang, F., Bartoo, M. L., Sellers, J. R., and Molloy, J. E. (2002) *Nat. Cell Biol.* **4,** 59–65
36. Baker, J. E., Krementsova, E. B., Kennedy, G. G., Armstrong, A., Trybus, K. M., and Warshaw, D. M. (2004) *Proc. Natl. Acad. Sci. U. S. A.* **101,** 5542–5546
37. Finer, J. T., Mehta, A. D., and Spudich, J. A. (1995) *Biophys. J.* **68,** suppl. 4, 291s–297s